Zoological Studies **59:**33 (2020)
doi:10.6620/ZS.2020.59-33

Zoological Studies

Special Issue: Fossil and Modern Clam Shrimp (Branchiopoda: Spinicaudata, Laevicaudata) Open Access

Population Density Effects on Carapace Growth in Clam Shrimp: Implications for Palaeontological Studies

Manja Hethke[1,*] and Stephen C. Weeks[2]

[1]*Institut für Geologische Wissenschaften, Freie Universität Berlin, Malteserstraße 74-100, D-12249 Berlin, Germany.*
**Correspondence: E-mail: manja.hethke@fu-berlin.de (Hethke)*
[2]*Department of Biology, The University of Akron, Akron, Ohio 44325-3908, USA. E-mail: scw@uakron.edu (Weeks)*

Received 30 January 2020 / Accepted 1 June 2020 / Published 5 August 2020

Special issue (articles 32-46) communicated by Thomas A. Hegna and D. Christopher Rogers

Fossil morphological data are time-averaged and generally reflect an overlap of different sources of carapace variability. To examine whether a proposed relationship between size and population density in fossil spinicaudatans is biologically meaningful, we set up rearing experiments involving two extant species: *Eulimnadia texana* and *Eocyzicus argillaquus*. Three and five days after hydration, clam shrimp were transferred into cups of various population densities that ranged between 1 and 15 inds/400 ml. Size and shape were measured 14 and 16 days after hydration, respectively. Every second day, we recorded length and sex of *E. texana*, which matured faster in lower-density cups. According to our growth model, population density and maximal carapace length follow a logarithmic relationship. At maturity, hermaphrodites yielded similar lengths across all population densities (~4.7 mm at 24°C), independent of age. Hence, clam shrimp can put off reproductive maturity as a response to decreased growth under higher density conditions. Growth rate generally decreases at maturity, but that effect is more pronounced in clam shrimp of high population densities, while low-density adults keep growing. For both species, multivariate analyses reveal that carapace size of low-density individuals is significantly larger than carapace size of higher-density individuals, while size values of intermediate densities cannot be distinguished. Shape distinction is strong in hermaphrodites of *E. texana*: 39.8% of the density-dependent shape variation is associated with relative umbo height, which is generally higher in individuals of smaller population densities. The *H/L* ratio, which is often used as a simple shape indicator, does not contribute to the main variation in shape, but it forms one of several ratios significant for 18.3% of the shape variability. In turn, the *H/L* ratio drives 30% of the shape variation in *E. argillaquus*. In addition, higher densities triggered shifts in ontogenetic growth trajectories in one third of the individuals, which led to aberrant morphologies. The present rearing experiment shows that some of the morphological variability on fossil bedding planes can be explained by population density. Also, it implies a considerable amount of ecophenotypic variability in Spinicaudata that affects our understanding of fossil taxonomy and palaeoecology.

Key words: Freshwater ecology, Morphometrics, Palaeontology, Phenotypic plasticity, Spinicaudata.

BACKGROUND

Lake environments witnessed major re-organizations during the Late Cretaceous to Paleogene, exemplified by a dramatic decline of spinicaudatan presence in the fossil record (Chen and Shen 1981; Gallego and Mesquita 2000; Astrop et al. 2015; Stigall et al. 2017). Studying the role of Spinicaudata in fossil lake ecosystems will be crucial for understanding that decline in diversity.

Citation: Hethke M, Weeks SC. 2020. Population density effects on carapace growth in clam shrimp: implications for palaeontological studies. Zool Stud **59:**33. doi:10.6620/ZS.2020.59-33.

To evaluate changes in fossil carapace size and shape through time, we require a sound understanding of intraspecific variability in extant species. Ontogenetic shape variability can be considerable in extant taxa (Brown et al. 2014), however, there is comparatively little information on ecophenotypic size and shape variability. Huang and Chou (2015 2017) reported strong temperature effects on developmental time and general life history traits in the androdioecious species *Eulimnadia braueriana* Ishikawa, 1895, including earliest hatching time and earliest maturation time; adaptations that may lead to niche differentiation between sympatric species.

Rearing experiments of the present study follow hypotheses based on palaeontological observations. Data that are easily obtainable during excavations are size and population density (number of specimens preserved on respective bedding planes by area). Such specimen counts predict a strong density effect on carapace size, as demonstrated by Wang et al. (2019) and Hethke et al. (2019) for the Middle Jurassic *Triglypta haifanggouensis* (Chen, 1976 in Zhang et al. 1976) and the Early Cretaceous *Eosestheria* cf. *middendorfii* (Jones, 1862). Low population densities correlate with large carapace sizes and vice versa.

However, such palaeontological observations are biased by time averaging and other sources of size and shape variation. Observed morphologies on bedding planes represent a combination of ontogenetic variability, sexual dimorphism, ecophenotypic variability, deformation, and species evolution. To evaluate whether the proposed density effect on morphology reflects a biologically meaningful relationship, we investigate the size and shape response to different population densities in two extant spinicaudatans: *Eulimnadia texana* (Packard, 1871) and *Eocyzicus argillaquus* (Timms and Richter, 2009).

MATERIALS AND METHODS

Rearing of *Eulimnadia texana* and *Eocyzicus argillaquus*

Population density effects on carapace growth have been examined by rearing two species of two different extant families. *Eulimnadia texana* (Limnadiidae) was reared from sediment collected by SCW in Arizona (USA; "Wallace" pool) in 2003 and *Eocyzicus argillaquus* (Eocyzicidae, per Schwentner et al. 2020) from sediment collected in Western Australia in 2007 (Cullimbin Pool 5). Rearing tanks and cups remained constantly lit under sunlight-simulating fluorescent bulbs (Duro-Test Corp.) and were kept in a windowless room air-conditioned to 24°C.

All individuals were reared under the same environmental conditions prior to their separation into cups of various population densities. Resting eggs of *Eulimnadia texana* were hydrated in a 10-gallon tank on 18 September 2017. Three days after hydration, we transferred 15, 10, 5, and 1 juveniles into 400 ml plastic cups (depth ~7.5 cm, diameter 8.3 to 11 cm), which were filled with wet-sieved (74 µm mesh size) aquarium water from an earlier (6-day old) branchiopod population reared from the same sediment. We replicated the experiment four times for single-individual cups, and twice for five- and ten-individual cups.

Eocyzicus argillaquus eggs were hydrated in a five-liter tank on 25 September 2017, and we recorded a huge hatch (50–75/liter) a day later. Hence, all individuals experienced comparatively high population densities during the first few days. Juveniles were transferred into 400 ml plastic cups on 30 September 2017 using sieved water from an earlier branchiopod population reared from Wallace sediments. We replicated single-individual cups four times, while 3-, 5-, 7-, 10-, and 15-individual cups were replicated twice. Carapace size and shape were measured once, 16 days after hydration.

Cup identifications indicate the initial density and the replicate (*e.g.*, cup 5.2 = initial density of 5, replicate 2). Cups were monitored daily for mortality, and dead individuals were removed and measured. We ended each experiment when mortality rate increased substantially. Depending on mortality rate, per-cup population densities decreased during the experiment. We considered the influence of individuals that died during the experiment on population density by standardizing density: Per-day population density was calculated by multiplying the initial population density with the proportion between the sum of days each individual remained alive in a cup and the potential number of days over all individuals (*i.e.*, if all individuals had survived). Example: initial density = 3, days = 4, and one individual found dead when the cup was examined on day 3 would result in a population density of $3\times(3+3+2+2)/12 = 2.5$. So, even though there were only eleven individuals of *Eulimnadia texana* remaining in cup 15 (= initial population density) 14 days after hydration, the standardized population density was a little higher: 12.75.

Growth (length) of 49 male and hermaphrodite *Eulimnadia texana* was measured 3, 5, 7, 9, 11, 14, and 16 days after hydration, resulting in a set of 282 measurements. Several individuals died during the experiment; 37 clam shrimp were still alive 14 days after hydration, while there were only 27 individuals

remaining two days later. To ensure an adequate sample size, we analysed size and shape of the 14-day old population. An Olympus microscope equipped with a COHU High Performance CCD Camera and the Scion Image software package were used for photography. To evaluate whether there was a population density effect on earliest maturation time, we documented sexual maturity during days of photography, resulting in a two-day resolution on maturation.

Each 400 ml cup was fed 1 ml of food per day [food mixture contained 0.5 g yeast and 0.5 g ground fish flake food (Tetramin) per 100 ml]. Hence, higher density cups received less food per individual.

Analytical methods

Possible effects of population density on growth were tested by collecting size and shape data for all surviving individuals 14 days (*Eulimnadia texana*) and 16 days (*Eocyzicus argillaquus*) after hydration (Tables S1–4). Population survival for *Eulimnadia texana* was recorded for an extra two days. Size and shape data for *Eulimnadia texana* was restricted to a hermaphrodite-only dataset (33 outlines), while *Eocyzicus argillaquus* is represented by both males and females (52 outlines). In a separate study, we analysed sexual dimorphism in *E. argillaquus*. For each specimen, we documented the valve outlined. Right valves were horizontally mirrored for shape analysis. Finally, we ordinated size and shape data using principal component analysis (PCA) on a variance-covariance matrix. To identify the number of meaningful PC shape variables, we used a scree plot that plots eigenvalues against a random model (Jackson 1993). Data analyses were carried out using the JMP Pro 14 package and the PAST software (version 3.24, folk.uio.no/ohammer/past/; Hammer et al. 2001).

Growth model for *Eulimnadia texana*

We fitted the growth data of each population density to a nonlinear function that can be used to model growth in organisms (von Bertalanffy: $y = a(1\text{-}be^{-cx})$; Brown and Rothery 1993). For each population density, the value of a represents an estimation of maximal carapace length according to the model (max. y).

Size (Linear measurements)

The size datasets in tables S1 and S3 each consist of nine linear variables (Fig. 1). While variable *Cr* was reconstructable for *Eocyzicus argillaquus*, it was not clear for *Eulimnadia texana*, for which we measured the distance from the dorsal margin to the highest point of the umbo (*u*). Size data has been log-transformed prior to PCA. PC axes have been interpreted by assessing associated eigenvector coefficients (loadings).

Shape

There is shape information in a multivariate dataset of linear measurements. It has been suggested to use Burnaby's method (Burnaby 1966) for size

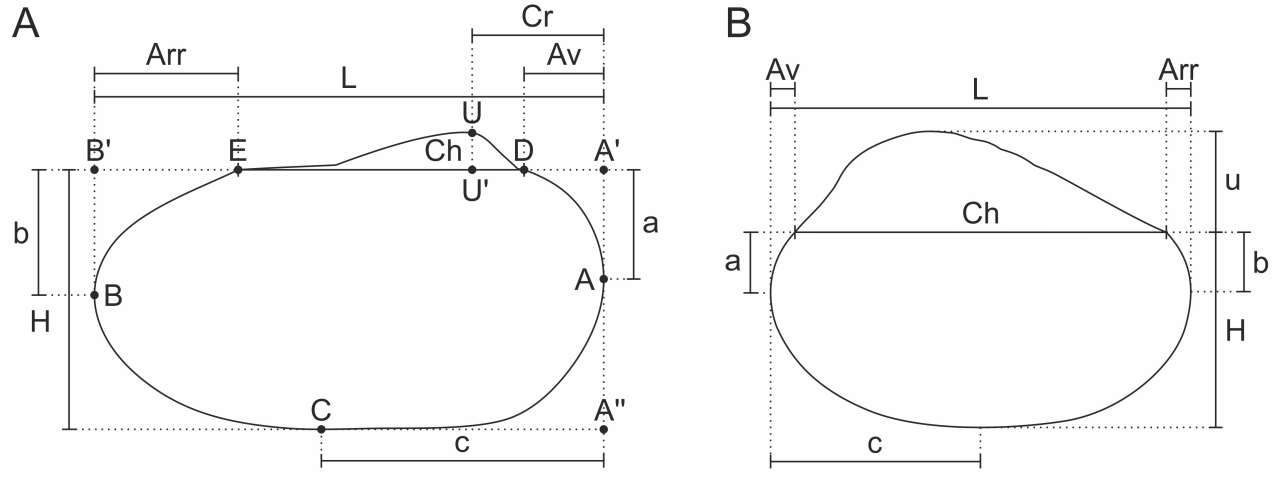

Fig. 1. Linear carapace variables used for A, *Eocyzicus argillaquus* and B, *Eulimnadia texana*, following Defretin-Lefranc (1965) and Tasch (1987): A, most anterior point of the valve; B, most posterior point of the valve; C, most ventral point of the valve; D, anterior extremity of the dorsal margin; E, posterior extremity of the dorsal margin; U, midpoint of the larval valve (located on the umbo, but not necessarily the midpoint of the umbo). *a*, vertical distance of A to A'; *b*, vertical distance of B to B'; *c*, horizontal distance of C to A"; *Arr*, horizontal distance of E to B'; *Av*, horizontal distance of D to A'; *Ch*, length of the dorsal margin; *Cr*, horizontal distance of U' to A'; *u*, vertical distance of Ch to highest point of the umbo; *L*, valve length; *H*, valve height.

correction (Rohlf and Bookstein 1987; Rohlf 1990; Hammer and Harper 2006), which eliminates variation parallel to *PC1* by projecting log-transformed measurements onto a plane orthogonal to this axis. This transformation should remove the size-dependent variation in a multivariate set of linear measurements.

A second method to explore shape is Fourier shape analysis (Crampton and Haines 1996; Haines and Crampton 2000). Outlines were transformed to 2000 xy-coordinates using the program tpsDig2 (version 2.31). Subsequently we used the program Hangle (Crampton and Haines 1996) to remove high frequency pixel noise that resulted from the automatic tracing of outlines by taking the weighted moving average over three coordinates (10 smoothing iterations). Hangle also performed the Fast Fourier Transform (FFT). As starting position, we chose the posterior extremity of the dorsal margin. A second program, Hmatch, normalized for starting position and orientation by minimizing the sums of the squares of all differences between the outlines (Haines and Crampton 2000). The highest order positive harmonic kept was 12, resulting in 22 shape variates (Fourier coefficients) for each specimen. In a final step, we projected the Fourier coefficient dataset (Tables S2 and S4) using principal component analysis (PCA).

To interpret the shape plots, we fitted bivariate datasets using ordinary least squares regression and explored whether the shape variables *PC1* and *PC2* (scores from PCA of Fourier coefficients) were linearly related to ratios $u/(u+H)$, H/L, and Ch/L. All residual plots have been checked for patterns indicating non-linear relationships.

Statistical testing

We used non-parametric MANOVA (NPMANOVA) to test whether clam shrimp of various population densities form statistically distinct morphological groups, based on Euclidean distances. NPMANOVA estimates the significance by permutation across groups (N = 9.999; Hammer and Harper 2006). An a-priori group consisted of all individuals of a specific population density in a 400 ml cup. Significant pairwise comparisons at $p < 0.05$ were shaded in according tables.

RESULTS

Eulimnadia texana Population survival

We ended the experiment 16 days after hydration. All single-density individuals and those in cup 5.2 survived, cup 5.1 went from a population density of 5 to 4.1 inds/400 ml, cup 10.1 to 9.3 inds/400 ml, cup 10.2 to 6.7 inds/400 ml and cup 15 to 12.1 inds/400 ml (Fig. 2A; Table 1A).

Eulimnadia texana Carapace length

According to the growth models in figures 2B and 3, the expected length in single-individual cups is 7.3 mm, while individuals of cup 15 reach

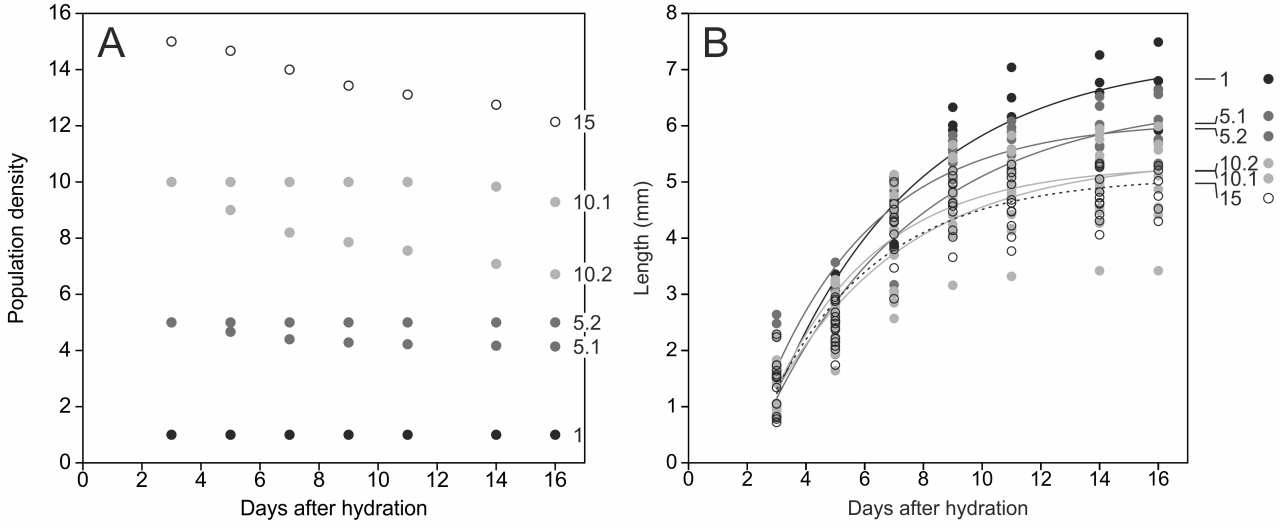

Fig. 2. *Eulimnadia texana* experiment (number of individuals = 49). Individuals were transferred into cups of various population densities three days after hydration (1, 5, 10 and 15 individuals/400 ml). A, Population survival. All individuals in cup 5.2 and in the four single-individual cups survived, while density declined fast in cups 10.2 and 15. B, Superimposed growth curves for all nine cups (compare with Fig. 3).

considerably smaller expected lengths of 5.1 mm. The superimposition of growth curves in figure 2B shows that maximal carapace lengths are ranked according to population density 16 days after hydration. Both, standardized population density and modelled maximal lengths are best fitted using natural log regression (Fig. 4A). In general, expected lengths decrease while population density increases. Also, the number of growth bands increases while length increases (Fig. 4B).

Length at maturity

A number of *Eulimnadia texana* hermaphrodites started carrying eggs on 25 September (seven days after hydration; Fig. 3). Two of three hermaphrodites were mature in cups 1.1–1.5, six of nine hermaphrodites in cups 5.1 and 5.2, and six of 15 hermaphrodites in cups 10.1 and 10.2 (Fig. 3). None of the clam shrimp in cup 15 were mature that day, implying a population density effect on earliest maturation time. Two days later, there was only one non-mature hermaphrodite in cup 15.

At earliest maturation time, average hermaphrodite lengths were 4.7 mm, 4.3 mm, 4.9 mm, 4.7 mm and 4.8 mm at 1.0, 4.4, 5, 10 and 8.2 inds/400 ml, respectively. On the same day, immature clam shrimp (hermaphrodites and males) of cup 15 yielded distinct average lengths of 4.1 mm. Nine days after hydration, hermaphrodites of cup 15 reached 4.7 mm (density: 13.43 inds/400 ml). At maturity, hermaphrodite length of different population densities cannot be statistically distinguished (Table S5). These data suggest average hermaphrodite body lengths of 4.7 mm at earliest maturation time (n = 23; at 24°C), based on a resolution of two days.

Eulimnadia texana

Size

PC1 and *PC2* explain 82.4% and 9.9% of the variance in the log-transformed size dataset. All nine linear variables have positive loadings on *PC1*, which are illustrated by vectors in the biplot of figure 5A. So, all variables increase towards positive scores of *PC1*, which can thus be regarded as a general size axis, although log-transformation added an aspect of

Table 1. Cup identification, initial density, and standardized population density. (A) *Eulimnadia texana*. (B) *Eocyzicus argillaquus*

(A) *Eulimnadia texana*

Cup ID	Initial density	Stand. density, 14 days	Stand. density, 16 days
1.1	1	1.00	1.00
1.3	1	1.00	1.00
1.4	1	1.00	1.00
1.5	1	1.00	1.00
5.1	5	4.17	4.14
5.2	5	5.00	5.00
10.1	10	9.83	9.29
10.2	10	7.08	6.71
15.1	15	12.75	12.14

(B) *Eocyzicus argillaquus*

Cup ID	Initial density	Stand. Density, 16 days
1.1	1	1.00
1.2	1	1.00
1.3	1	1.00
1.4	1	1.00
3.1	3	2.75
3.2	3	2.58
5.1	5	4.83
5.2	5	4.42
7.1	7	6.58
7.2	7	6.25
10.1	10	9.33
10.2	10	9.50
15.1	15	14.00
15.2	15	13.83

shape. Figure 5A also shows that specimens in cup 15 (= population density of 12.8 inds/400 ml, 14 days after hydration) mostly occupy negative scores on *PC1* while single-individual cups (red) occupy positive scores on *PC1*. Hence, size in high-density cups is generally smaller than in low-density cups. Specimens of intermediate population densities occupy intermediate areas along *PC1*. Both, *PC1* and *PC2*, are driven by *Av*, while *PC2* is also strongly influenced by variables *Arr* and *u*.

NPMANOVA of log-transformed linear measurements indicates that differences in size are significant across different population densities (Table 2A; *p*(same) = 0.0002). However, pairwise comparisons reveal that only density extremes (cups 1 and 15) yield significantly different carapace sizes compared to other population densities. Intermediate densities cannot be separated. In comparison to length (Fig. 4), size (*PC1* scores) by population density can also be well fitted by a linear relationship for *Eulimnadia texana* (Fig. S1; that of *Eocyzicus argillaquus* is best fitted by a logarithmic relationship).

During the outlining process, we noticed that the anterior dorsal extremity (landmark D in Fig. 1), which highly influences values of *Av*, was sometimes difficult to identify. Hence, we carried out a second analysis with a reduced set of log-transformed linear measurements (*H*, *L*, *Ch*, *u*) that resulted in an overall similar plot, except that *PC2* now explained a larger proportion of the variance in the dataset (17.1%). All four variables drive *PC1* at almost equal proportions. *H*, *L*, and *Ch* increase towards positive scores of *PC2* while *u* decreases. In general, there seems to be little difference between the analyses of nine and four linear variables. NPMANOVA yielded almost the same result except for one pairwise comparison (cups 15 and 10.1) that cannot be statistically distinguished in table 2B.

Eulimnadia texana

Shape

According to Fourier shape analysis (PC of Fourier coefficients in figure 5B, NPMANOVA in Table 3), there is an overall significant population density effect on carapace shape (*p*(same) = 0.0001). Nine of fifteen pairwise comparisons exhibit significantly different shapes. Most non-significant comparisons can be explained by similar population densities 14 days

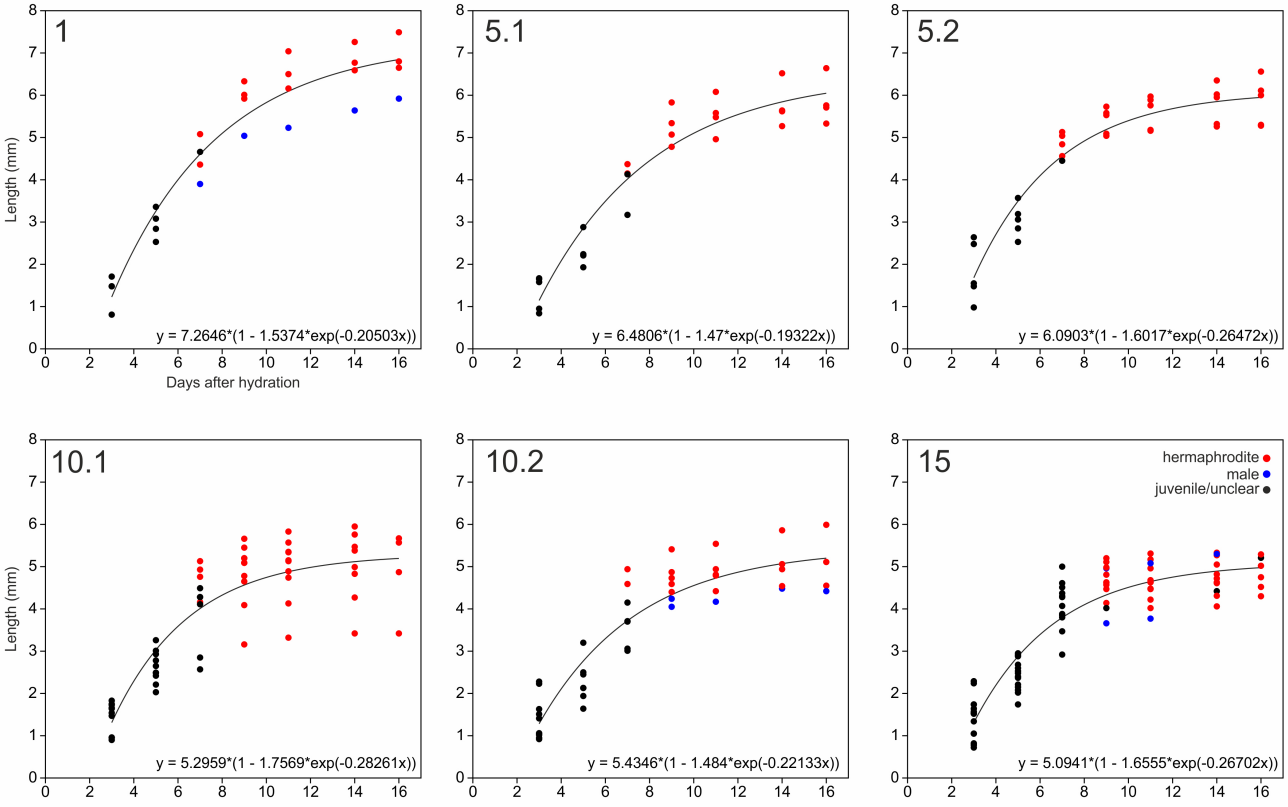

Fig. 3. *Eulimnadia texana* experiment, $n = 282$. Growth model curves follow the von Bertalanffy equation $y = a(1\text{-}be^{-cx})$. The value of *a* represents an estimation of maximal length (max. *y*). Colours represent hermaphrodites (red), males (blue), and juvenile or unclear (black). Numbers in upper left corner represent initial population density and replicate.

after hydration, except for two comparisons that include cup 10.2 (density 7.1 inds/400 ml), for which the *p*-value is, however, close to the significance level (set to α = 0.05).

Eigenvalues plotted against a random model (scree plot) resulted in two significant components. *PC1* and *PC2* explain 39.8% and 18.3% of the variance in the Fourier dataset (Fig. 5B). Extreme shapes along *PC1* indicate a much larger relative umbo height in low-density cups (Fig. 6).

The shape plot can be further interpreted using ordinary least squares regression of *PC1* and *PC2* scores versus ratios *u*/(*u*+*H*), *H*/*L*, *Ch*/*L* (Fig. 7). According to figure 7A–C, *PC1* is driven by relative umbo height, while the regression is not significant for the *H*/*L* ratio. Hence, the main difference in shape is not described by the *H*/*L* ratio, which is often used as a simple shape indicator for clam shrimp. But it forms one of several

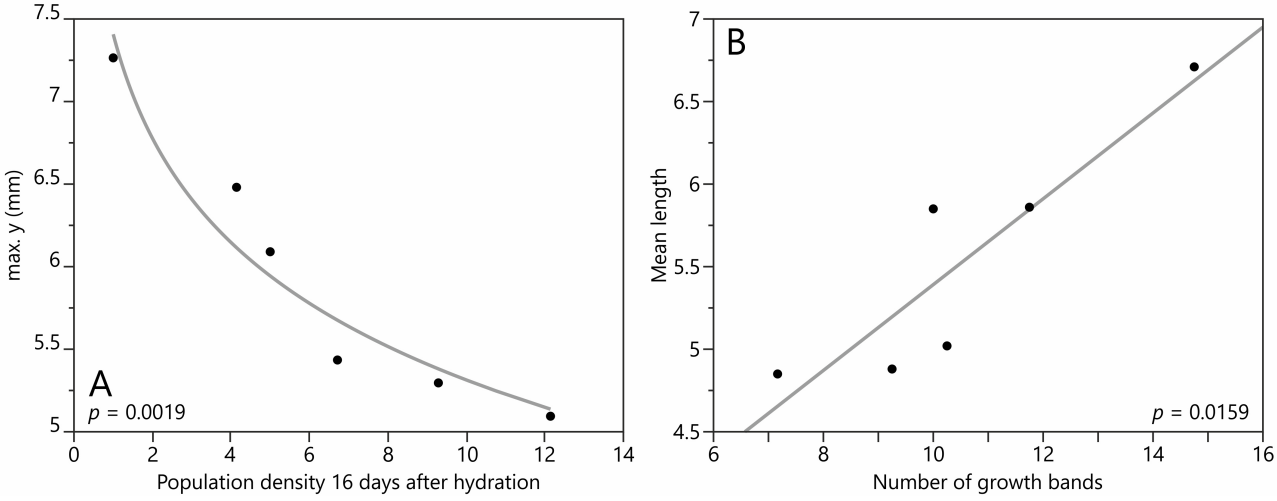

Fig. 4. A, Bivariate fit of max. *y* (estimated from von Bertalanffy equation) by standardized population density 16 days after hydration. Natural log regression provides the best fit. B, Bivariate fit of mean length by mean number of growth bands (per cup).

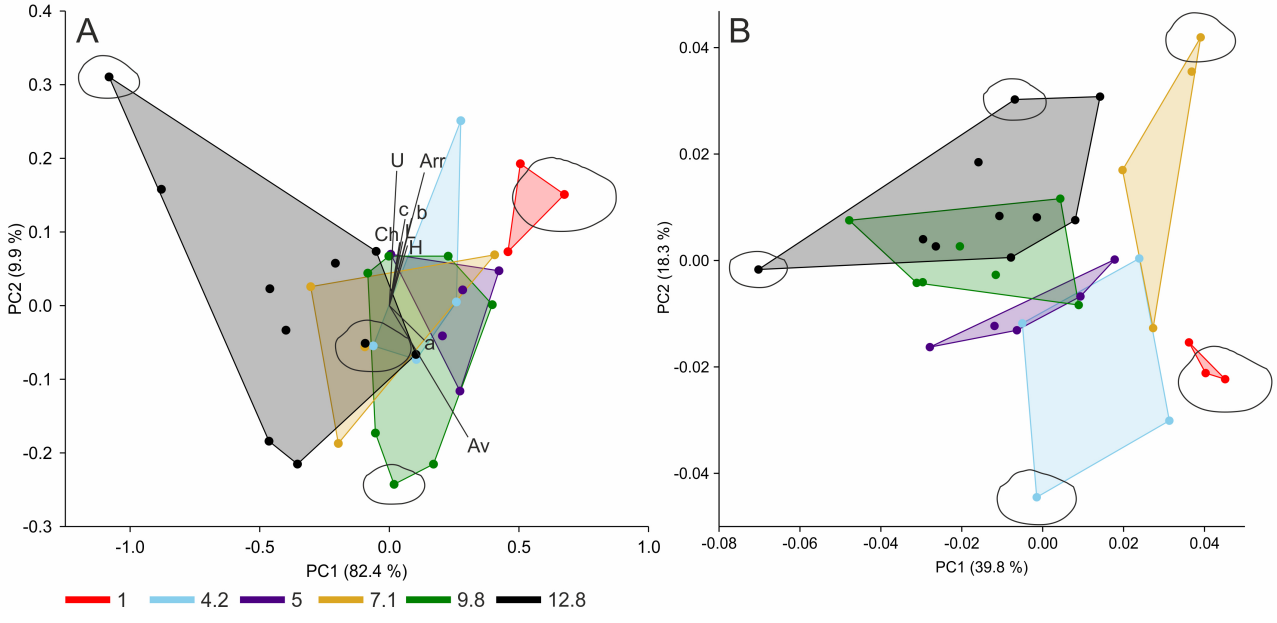

Fig. 5. Population density effect on size and shape in *Eulimnadia texana*. Colours represent standardized population densities 14 days after hydration that range between 1 and 12.8 individuals/400 ml. A, Biplot of principal component scores and variable vectors (loadings) on *PC1* and *PC2* of a set of log-transformed linear measurements. B, Fourier shape analysis. Although the analysis is shape-only, outlines have been scaled to size for better comparison with the size plot. *PC1* represents relative umbo size, while *PC2* is driven by several ratios, including the *H*/*L* ratio and relative size of the dorsal margin (compare with Fig. 7).

ratios driving *PC2* (Fig. 7E; $p < 0.001$). *PC2* is also influenced by relative length of the dorsal margin (Fig. 7F), with generally shorter dorsal margins compared to length in low-density cups.

Burnaby transformation of linear measurements

In contrast, NPMANOVA of the multivariate size dataset that has been transformed using Burnaby's method did not yield overall statistically distinct groups

Table 2. Non-parametric MANOVA of log-transformed linear measurements of *Eulimnadia texana*. Summary and pairwise comparisons. Significant pairwise comparisons ($p < 0.05$) are shaded. Pairwise comparisons reveal that linear measurements of density extremes (cups 1 and 15) are generally distinct. Intermediate densities cannot be statistically distinguished. (A) Nine linear variables. (B) Four linear variables

(A) NPMANOVA of nine linear variables, log-transformed (*E. texana*)					
Permutation N:		9999			
Total sum of squares:		5.736			
Within-group sum of squares:		2.693			
F:		6.102			
p (same):		0.0002			
Pairwise comparisons					
	5.1	5.2	10.1	10.2	15
1	0.0558	0.0153	0.0077	0.0581	0.0028
5.1		0.5639	0.3263	0.2841	0.0206
5.2			0.2106	0.1098	0.0043
10.1				0.3471	0.005
10.2					0.1195
(B) NPMANOVA of four linear variables *Ch*, *u*, *H*, *L*, log-transformed (*E. texana*)					
Permutation N:		9999			
Total sum of squares:		0.6789			
Within-group sum of squares:		0.3047			
F:		6.632			
p (same):		0.0001			
Pairwise comparisons					
	5.1	5.2	10.1	10.2	15
1	0.0881	0.0179	0.018	0.0553	0.0041
5.1		0.6958	0.1082	0.1143	0.001
5.2			0.146	0.0766	0.0012
10.1				0.1662	0.1541
10.2					0.0779

Table 3. Non-parametric MANOVA of Fourier coefficients of *Eulimnadia texana.* Significant pairwise comparisons ($p < 0.05$) are shaded. Differences in shape are significant across different population densities (p(same) = 0.0001), reflected by multiple significant pairwise comparisons of intermediate population densities

NPMANOVA of Fourier coefficients (*E. texana*)					
Permutation N:		9999			
Total sum of squares:		0.06027			
Within-group sum of squares:		0.0361			
F:		3.616			
p (same):		0.0001			
Pairwise comparisons					
	5.1	5.2	10.1	10.2	15
1	0.0871	0.0174	0.009	0.0595	0.0035
5.1		0.4317	0.0249	0.0578	0.0021
5.2			0.1956	0.0241	0.0413
10.1				0.0038	0.3472
10.2					0.0065

(Table 4; p(same) = 0.218). Pairwise comparisons reveal just one significant pair (cups 1 and 10.1). Hence, shape variation between hermaphrodites of different population densities is too subtle to use this method for shape discrimination.

Eocyzicus argillaquus
Population survival

Standardized densities of replicates in *Eocyzicus argillaquus* did not diverge much (Fig. 8, Table 1B). Survival remained at 100% until 10 days after hydration.

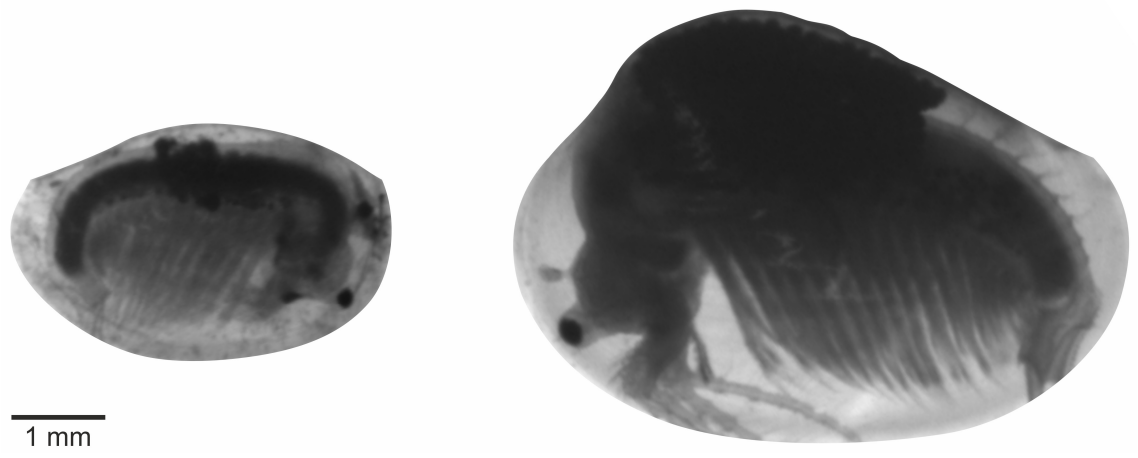

Fig. 6. Size and shape variation in *Eulimnadia texana*. Pictured are the two extreme shapes that represent the most negative and most positive scores on *PC1* in figure 5B. Individuals have been scaled to size (population densities of 12.8 individuals/400 ml, left, and 1 individual/400 ml, right; individuals 15.1_6 and 1.1_1).

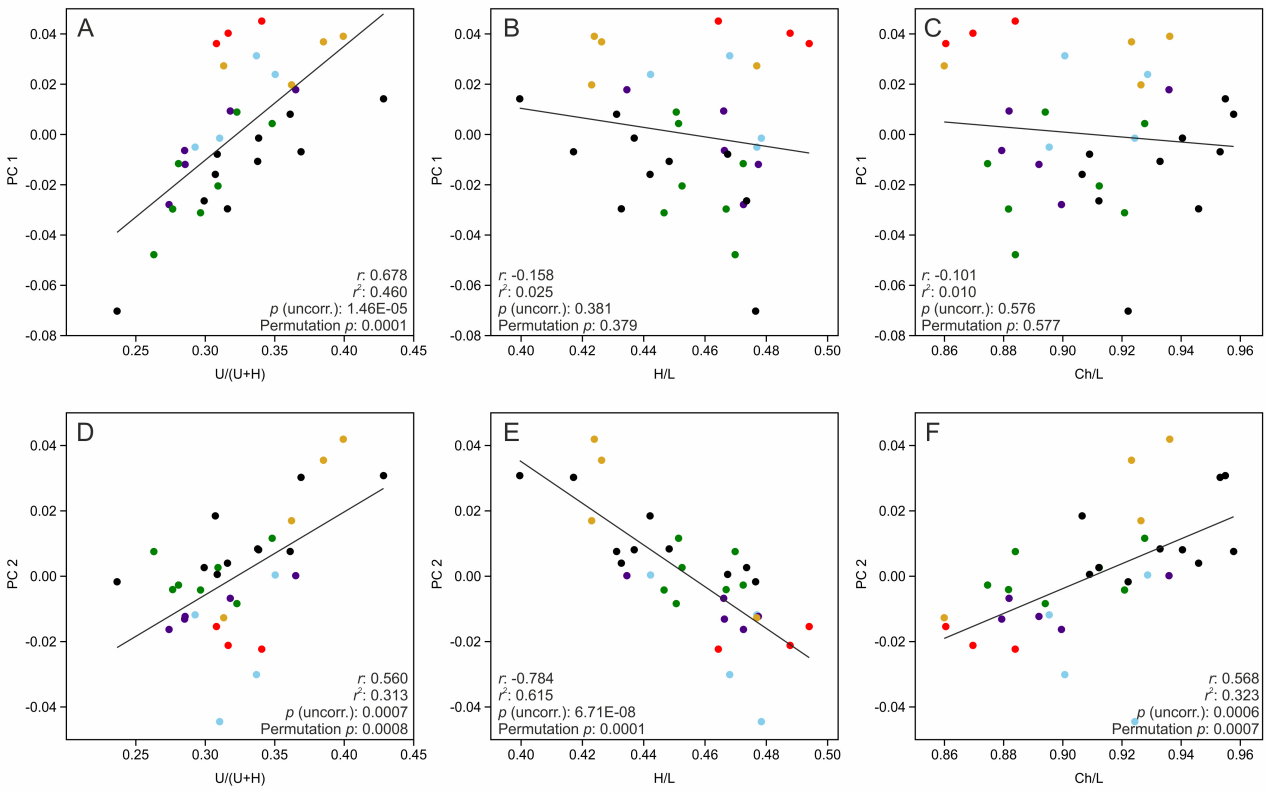

Fig. 7. Ordinary least squares regression of *PC1* and *PC2* scores of the Fourier shape analysis in figure 5B versus ratios $u/(u+H)$, H/L, Ch/L. Shape change in *PC1* is correlated with higher $u/(u+H)$ ratios. The H/L ratio does not drive *PC1*, but it contributes to *PC2*.

Population densities first started to decrease in cups 15.1 and 15.2 eleven days after hydration, followed by cups of lower densities 13 days after hydration. We decided to end the experiment when mortality rate increased dramatically 16 days after hydration. To ensure a statistically relevant sample size, we pooled replicates 3, 5, 7, and 10 for further analyses (*e.g.*, only one individual remaining in cup 3.2).

Eocyzicus argillaquus
Size

PC1 and *PC2* explain 76.0% and 12.6% of the variance in the log-transformed size dataset. Figure 9A shows that single-individual cups (in red) occupy positive scores on *PC1* while all other densities overlap, which is corroborated by NPMANOVA (Table 5A). Pairwise comparisons separate single-individual cups from cups with initial densities higher than three. Cup 3 is distinct from cups 5 and 15.2. All other cups cannot be distinguished based on size variables. So, in contrast to *Eulimnadia texana*, the population density effect on size in *E. argillaquus* mostly affects very-low density cups rather than density extremes. Further studies might reveal whether densities higher than 14 inds/400 ml yield distinct size patterns. All linear variables have positive loadings on *PC1* (size variable), and size in higher-density cups is generally smaller than in single-individual cups. *PC2* is driven by variable *c*. High *c* values often indicate aberrant forms, such as the specimen illustrated in figure 10D.

The analysis of the five variables that were easiest to obtain (Table 5B) provides similar results, which shows that it is not essential to worry about variability in linear variables during data acquisition. Also, *PC1* (as a measure of size) by population density is best fitted by a logarithmic relationship in *E. argillaquus* (Fig. S1).

Eocyzicus argillaquus
Shape

PC1, *PC2*, and *PC3* explain 30.0%, 18.3%, and 14.1% of the variance in the Fourier dataset (Fig. 9B, Table S4, Fig. S2). Ordinary least squares regression of *PC1* and *PC2* scores versus *H*/*L* (Fig. 11) indicates that *PC1* is driven by that ratio (compare specimens in Fig. 10A and B). According to Fourier shape analysis (NPMANOVA in Table 6), there is an overall significant population density effect on carapace shape (p(same) = 0.0021). However, that difference in shape is driven by

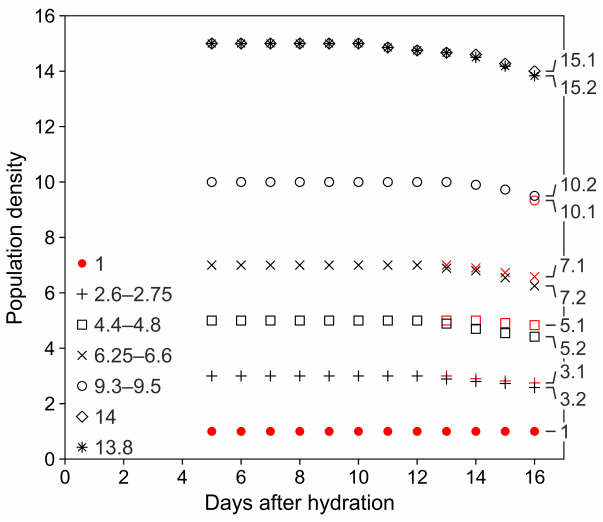

Fig. 8. Population survival of *Eocyzicus argillaquus*. Five days after hydration, individuals were transferred into 400 ml cups and survival was monitored daily. Population densities remained initially stable and started to decline in cups 15.1 and 15.2 eleven days after hydration. We ended the experiment when raw densities dropped notably (29 of 84 individuals dead on 11 October 2017). Numbers in the legend represent standardized population densities 16 days after hydration.

Table 4. Non-parametric MANOVA of a multivariate set of linear measurements of *Eulimnadia texana* transformed using Burnaby's method. Summary and pairwise comparisons. Significant pairwise comparisons ($p < 0.05$) are shaded

NPMANOVA of linear measurements transformed using Burnaby's method (*E. texana*)					
Permutation N:	9999				
Total sum of squares:	1.008				
Within-group sum of squares:	0.8118				
F:	1.306				
p (same):	0.2184				
Pairwise comparisons					
	5.1	5.2	10.1	10.2	15
1	0.3405	0.0554	0.0225	0.0875	0.2425
5.1		0.6865	0.1315	0.2636	0.4781
5.2			0.3824	0.2517	0.9272
10.1				0.2688	0.5539
10.2					0.2876

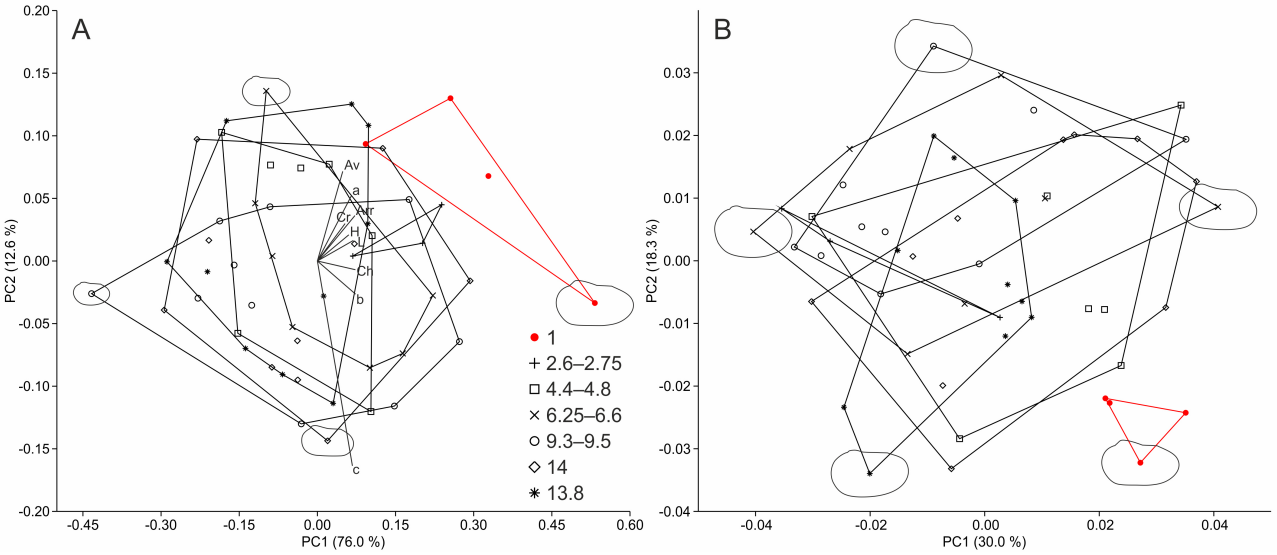

Fig. 9. Population density effect on size and shape in *Eocyzicus argillaquus*. A, Biplot of principal component scores and variable vectors (loadings) on *PC1* and *PC2* of a set of log-transformed linear measurements. Outlines scaled to size. B, Population density effect on shape in *Eocyzicus argillaquus* based on Fourier shape analysis. Outlines represent shape only.

Table 5. Non-parametric MANOVA of log-transformed linear measurements of *Eocyzicus argillaquus*. Summary and pairwise comparisons. Significant pairwise comparisons ($p < 0.05$) are shaded. (A) Nine linear variables. (B) Five linear variables

(A) NPMANOVA of nine linear variables, log-transformed (*E. argillaquus*)						
Permutation N:		9999				
Total sum of squares:		2.283				
Within-group sum of squares:		1.64				
F:		2.872				
p (same):		0.0058				
Pairwise comparisons						
	3	5	7	10	15.1	15.2
1	0.2532	0.0105	0.0178	0.0075	0.006	0.0011
3		0.0358	0.1191	0.0892	0.0584	0.0182
5			0.5571	0.5891	0.7414	0.8284
7				0.4114	0.5084	0.3124
10					0.8359	0.7618
15.1						0.8929
(B) NPMANOVA of five linear variables *Arr*, *Ch*, *Cr*, *H*, *L*, log-transformed (*E. argillaquus*)						
Permutation N:		9999				
Total sum of squares:		1.149				
Within-group sum of squares:		0.7774				
F:		3.506				
p (same):		0.0021				
Pairwise comparisons						
	3	5	7	10	15.1	15.2
1	0.1116	0.0049	0.0089	0.0036	0.0051	0.0006
3		0.0673	0.1026	0.0967	0.1373	0.0481
5			0.7646	0.5304	0.9917	0.8125
7				0.3825	0.6888	0.4645
10					0.5586	0.5795
15.1						0.8576

the distinct shape of clam shrimp in single-individual cups, reflecting the size results in table 5.

Burnaby transformation of linear measurements

NPMANOVA of the multivariate size dataset that has been transformed using Burnaby's method was not distinct (Table 7; p(same) = 0.1275), with only two

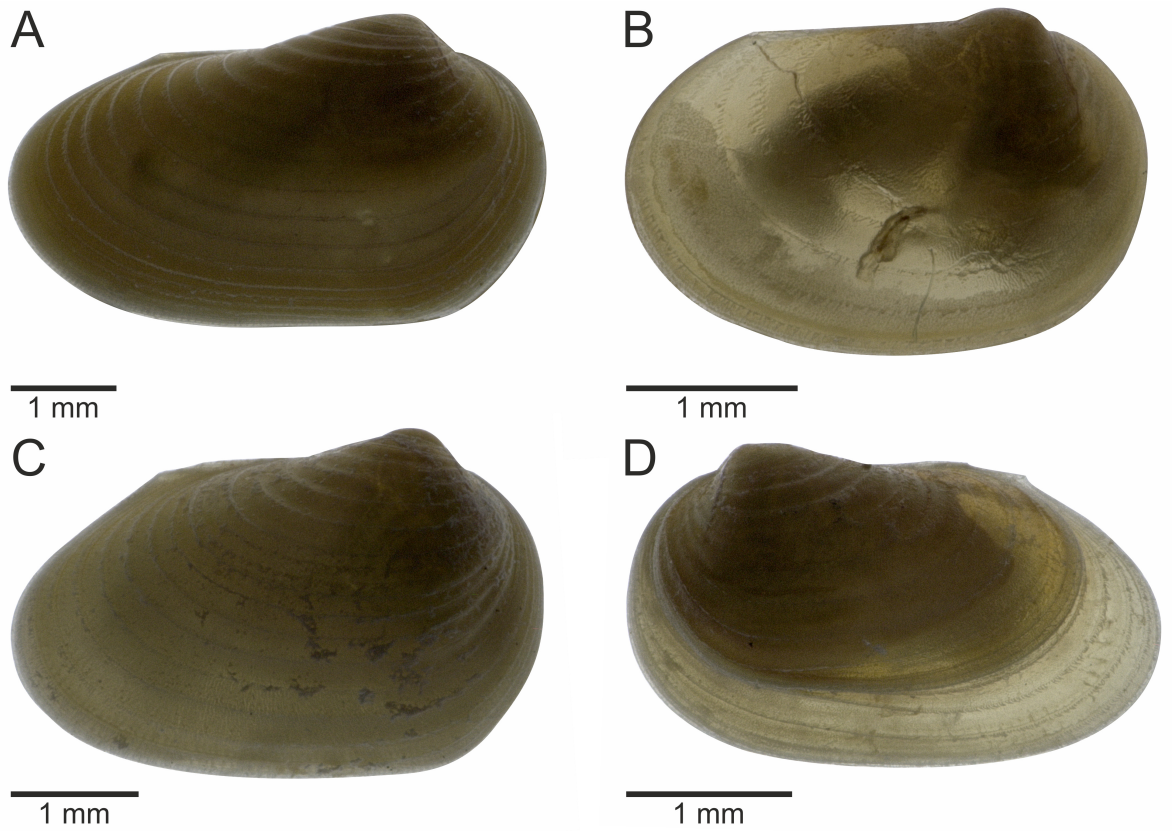

Fig. 10. Shape dependency on population density in *Eocyzicus argillaquus*. A–D, 1.1_1 (1 inds/400 ml), 7.1_3 (6.6 inds/400 ml), 15.1_6, 15.1_7 (both 14 inds/400 ml). A and B, Shape variable *PC1* in figure 9B represents the difference between elongate and more oval carapaces (= positive and negative scores along *PC1*, respectively). C, 14.1% of the shape variability (*PC3*; Fig. S1) represents the difference between an oval and a subquadratic outline (shown here). D, Aberrant growth affected one third (7/21) of the photographed clam shrimp in cups 15.1 and 15.2. A shift in growth modified carapace proportions and the dorsal margin.

Table 6. Non-parametric MANOVA of Fourier coefficients of *Eocyzicus argillaquus*. Summary and pairwise comparisons. Significant pairwise comparisons ($p < 0.05$) are shaded

NPMANOVA of Fourier coefficients (*E. argillaquus*)						
Permutation N:	9999					
Total sum of squares:	0.07935					
Within-group sum of squares:	0.0633					
F:	1.859					
p (same):	0.0021					
Pairwise comparisons						
	3	5	7	10	15.1	15.2
1	0.0251	0.0031	0.0174	0.0005	0.0157	0.0008
3		0.0681	0.4206	0.2509	0.2102	0.2091
5			0.347	0.0392	0.7141	0.313
7				0.7428	0.5505	0.3265
10					0.1812	0.2729
15.1						0.491

significant pairwise comparisons (cups 10 and 1; 10 and 3). Fourier shape analysis seems superior for shape discrimination in clam shrimp.

Size and shape comparison

We tested the overprint of population density on inter-species variability by combining the size and shape datasets, respectively. In the size analysis (Fig. 12A), *PC1* (75.2%) discriminates between the two species, whereas the population density effect on size is mostly picked up by *PC2* (19.2%). Also, size variation is larger in *Eulimnadia texana* than in *Eocyzicus argillaquus*. Inter-species shape distinction is even more pronounced (Fig. 12B); *PC1* (86.6%) represents the distinction between two species whereas the population density effect on shape is only represented by higher principle components. The perfect distinction between the two species is due to inter-family size and shape variability. Intra-family variability will be subtler.

DISCUSSION

Population density effects on life history traits in *Eulimnadia texana*

Earliest maturation time

There are strong temperature effects on life history traits in the limnadiid *Eulimnadia braueriana*: Earliest maturation times vary significantly and take 18.3 +/- 4.7 days at 15°C but only 5.3 +/- 0.6 days at 30°C (Huang and Chou 2015 2017). Weeks et al. (1999) also noted that inbred *E. texana* mature ~1 day later than their more heterozygous counterparts (6.9 vs. 5.6 days).

In the present study, *Eulimnadia texana* hermaphrodites carried their first eggs seven days after hydration (25 September; Fig. 3). Two days later, eleven of twelve individuals in cup 15 were mature (2 males and 9 hermaphrodites), implying a population density effect on earliest maturation time in *E. texana*. Mature individuals were commonly larger than non-mature individuals of the same cup on 25 September (Fig. 3). At maturity, hermaphrodites yielded average lengths of 4.7 mm across all population densities but on different days (under 24°C). Hence, clam shrimp can put off reproductive maturity as a response to decreased growth under higher density conditions. So, the population density effect on maturity is of indirect nature and connected to size.

Huang and Chou (2015 2017) reached somewhat similar conclusions in their temperature studies. At maturity, there was no significant difference in body length of *Eulimnadia braueriana* under different temperature treatments, so Huang and Chou (2015) conclude that temperature affects developmental time rather than body length. However, figure 1 in Huang and Chou (2017) suggests that temperature affects size. Estimated body lengths at earliest maturation time were 2.3 mm, 2.7 mm, 3.2 mm, and 2.9 mm under 15, 20, 25, and 30°C, respectively.

Survival rate

Survivorship in *Eulimnadia braueriana* reduced faster at higher temperatures, attributed to reduced oxygen availability, yet the maximum lifespan (death of last individual under a specific temperature) was independent of temperature (Huang and Chou 2015).

The survival rate in *Eulimnadia texana* was substantially reduced in higher-density cups (10.1, 10.2 and 15) 16 days after hydration (standardized survival in figure 2A; raw survival in Fig. S3). The average lifespan of *E. texana* is 10 to 15 days (Weeks et al. 1997; Zucker et al. 2001; Weeks and Bernhardt 2004; Weeks et al. 2014), with a fairly constant mortality rate between 10 and 22 days (Weeks et al. 1997). Males live 1 to 2 days less, on average, than hermaphrodites (Zucker et al. 2001; Weeks and Bernhardt 2004), with the difference between male and hermaphrodite survival lessening as mating opportunities increase (Zucker et al. 2001; Weeks et al. 2014).

Population density versus sexual dimorphism in *Eocyzicus argillaquus*

Eocyzicus argillaquus is sexually dimorphic, which is common in clam shrimp (Weeks et al. 2006), but there is considerable overlap in male and female morphospace (pers. obs.). To estimate the degree of according size and shape overprint, we targeted sexual dimorphism in *E. argillaquus* in a separate analysis. Individuals were kept in separate cups at 24°C, and the analysis was ended 21 days after hydration.

Shape dimorphism is subtle (but statistically significant), with considerable overlap in shape space; mean male and mean female shapes are illustrated in figure S4. In contrast, length separation (Fig. S5) is distinct with females growing faster than males. Carapace lengths of dimorphs started to diverge when clam shrimp were about 12 to 13 days old, so we expect size dimorphism in the 15-day old clam shrimp of the present study.

This dimorphism certainly led to a mixed signal of sexual dimorphism and population density effects in the present study. Nevertheless, figure 9 corroborates a population density effect on size and shape in *Eocyzicus*

argillaquus (Table 5): Carapaces in single-individual cups (in red) are more elongate and larger (small *H/L*, Figs. 10A, 11), while sexual dimorphism can be characterized by more elongate but distinctly smaller males.

Population density and aberrant growth in *Eocyzicus argillaquus*

Some of the size and shape variation in higher-density cups derives from aberrant growth (Fig. 10D). Shifts in growth trajectories during ontogeny led to a change in overall carapace proportion, which is picked up by *PC2* in the size analysis of figure 9A. The clam shrimp reacted to increased crowding by providing more space in the posterior part of the carapace, which increased size variable *c*. Specimens with long *c* are represented by the most negative scores along *PC2* in the size analysis of figure 9A. Hence, that shift in growth accounts for 12.6% of the variability in the size dataset. Such shifts also affect the dorsal margin; it appears as if the carapace was rotated relative to growth increments of earlier ontogenetic stages. Aberrant growth is present in seven of 21 clam shrimp of cups 15.1 and 15.2, and in six of 27 clam shrimp of cups 5 to 10. Clam shrimp of cups 1 and 3 were not affected.

Fossil observations corroborated by rearing experiments

Lower densities triggering fast carapace growth have been proposed for clam shrimp of the

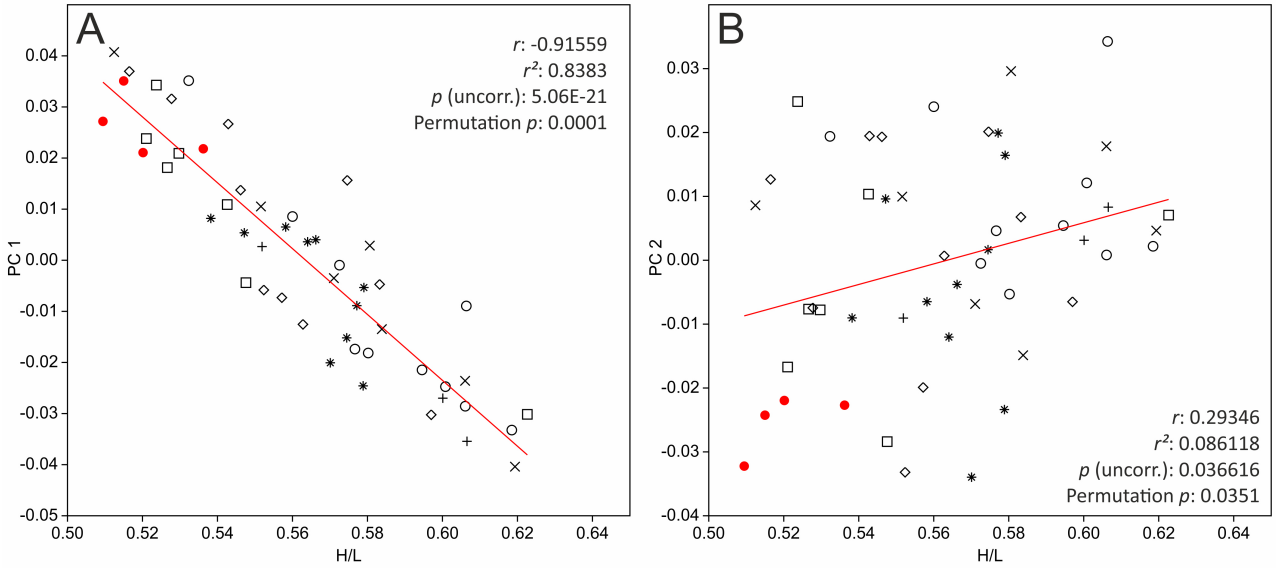

Fig. 11. A, B, Ordinary least squares regression of *PC1* and *PC2* scores (shape analysis) by the *H/L* ratio, which drives shape variable *PC1*.

Table 7. Non-parametric MANOVA of a multivariate set of linear measurements of *Eocyzicus argillaquus* transformed using Burnaby's method. Summary and pairwise comparisons. Significant pairwise comparisons ($p < 0.05$) shaded

NPMANOVA of linear measurements transformed using Burnaby's method (*E. argillaquus*)						
Permutation N:	9999					
Total sum of squares:	0.5468					
Within-group sum of squares:	0.458					
F:	1.423					
p (same):	0.1275					
Pairwise comparisons						
	3	5	7	10	15.1	15.2
1	0.111	0.5745	0.1202	0.0158	0.0847	0.2311
3		0.2041	0.2352	0.0417	0.0501	0.0785
5			0.5433	0.1576	0.3397	0.6481
7				0.727	0.3946	0.3977
10					0.6302	0.2757
15.1						0.7286

Middle Jurassic Haifanggou Formation (*Triglypta haifanggouensis*, Yanliao Biota; Wang et al. 2019) and the Lower Cretaceous Yixian Formation (*Eosestheria* cf. *middendorfii*, Jehol Biota; Hethke et al. 2019), with linear fit and natural log regression providing the better fit, respectively. Linear fit also provides the better fit for clam shrimp of the Late Jurassic Tiaojishan Formation (*Liaoxiestheria linglongtaensis*, Yanliao Biota; Jan Schmidt, MH pers. obs., bivariate fit of mean length by density in Fig. S6).

The analysis of population density effects in fossil material should involve an evaluation of time averaging that can be achieved by counting the number of submillimetric layers. Investigations of fossil pavements from the Yixian Formation of western Liaoning include spinicaudatans from one to four closely adjacent layers. Hence, the examined fossil size distributions (uni-, bi- or polymodal) often reflect an overlap of consecutive populations; yet mean size and population density are nevertheless correlated. Spinicaudatan densities of *Triglypta haifanggouensis* range between 0.9 and 144.9 inds/100 cm^2 (1 and 2 layers, respectively; Wang et al. 2019). In the case of the Early Cretaceous *Eosestheria* cf. *middendorfii*, we counted 0.01 to 255.4 specimens per 100 cm² (Supplementary material S3 of Hethke et al. 2019; the two outliers of 694 and 1066 inds/100 cm^2 represent juvenile mass mortality events).

Translating such two-dimensional data into actual population densities is difficult. For example, 255.4 inds/100 cm^2 of *E.* cf. *middendorfii* were counted on a bedding plane that consisted of two closely adjacent layers. Assuming little or no post-mortem transport, the count represents a time-averaged estimate of two successive clam shrimp populations living in the water column above 100 cm^2. For comparison, the cups of the present study yield areas of about 50 cm^2 (bottom) to 95 cm^2 (top), so cups 1 to 15 represent densities of ~1 to 30 inds/100 cm^2, within the range reported for fossil bedding planes. 23 of 41 bedding planes that contain spinicaudatan fossils yield densities of less than 10 inds/100 cm^2. Such exceptionally low population densities correlate with exceptionally large carapaces in all cases (example bedding plane H: 2.3 inds/100 cm^2, 2 layers, L = 18.02 on average; Hethke et al. 2019), a pattern corroborated by the rearing experiments of the present study (Figs. 5, 9). Hence, population density affected fossil clam shrimp growth, mediated by higher nutrient availability and, accordingly, less competition for resources.

CONCLUSIONS

The rearing experiments of the current study corroborate a relationship between carapace length and population density in fossil morphological data. The response of carapace length to population density in

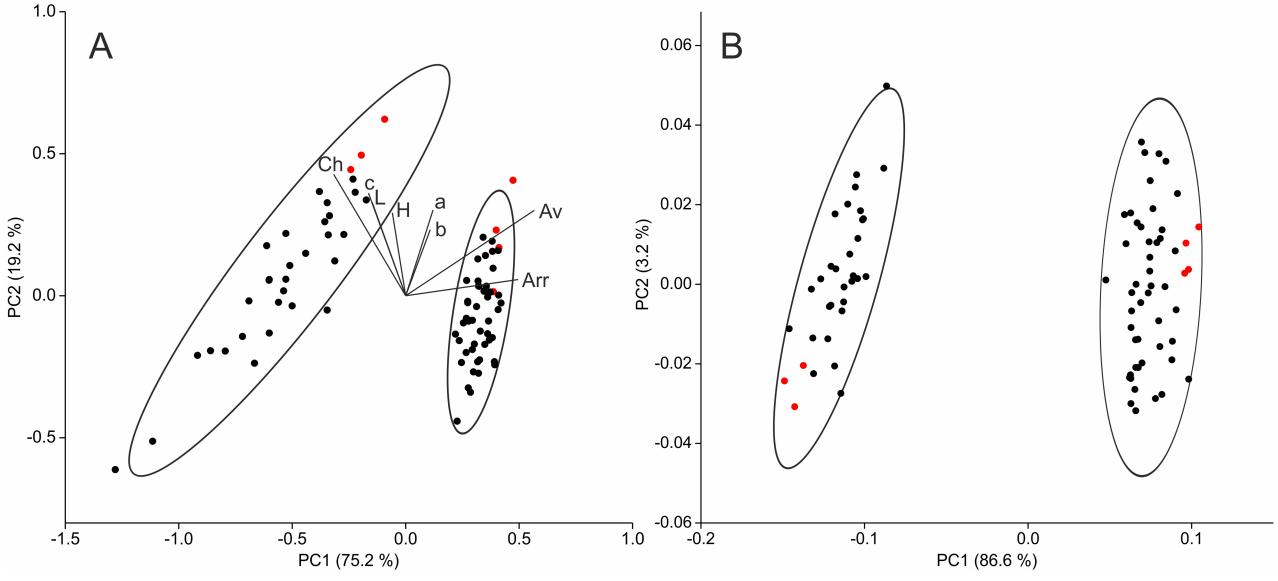

Fig. 12. Comparison of size and shape morphospaces. Red dots represent single-individual cups. A, Biplot on *PC1* and *PC2* of eight log-transformed linear variables. 95% concentration ellipses show that size analysis separates both species well: *Eulimnadia texana* occupies negative values on *PC1*, while *Eocyzicus argillaquus* occupies positive values on *PC1*. *Eulimnadia texana* is driven by larger Ch values (dorsal margin) and *Eocyzicus argillaquus* by larger *Av* and *Arr* values. B, Biplot on *PC1* and *PC2* of the combined Fourier datasets. *Eulimnadia texana* occupies negative values on *PC1*, while *Eocyzicus argillaquus* occupies positive values on *PC1*. The density effect is represented by *PC2*.

Eulimnadia texana follows a logarithmic relationship, with lower densities triggering faster growth. In addition, *Eulimnadia texana* seems to mature faster in lower-density cups. At maturity, hermaphrodites yield similar lengths across all population densities but on different days. Subsequently, the growth rate of high-density clam shrimp strongly decreases, leading to maximal lengths that are only a little larger than length at maturity, while low-density clam shrimp keep growing.

There is a significant effect of population density on size (defined as a combination of several linear variables). Low population densities are represented by larger carapaces in both species, *Eulimnadia texana* and *Eocyzicus argillaquus*. For data acquisition, it is not essential to worry about variability in linear variables, as robust variables yield similar results as the analysis of the full set of linear measurements. In addition, there is a strong density effect on hermaphrodite shape in *Eulimnadia texana*: low-density hermaphrodites yield larger relative umbo heights. The population density effect on shape in *Eocyzicus argillaquus* is less pronounced, yet significant for single-individual cups that yield smaller *H/L* ratios than clam shrimp of higher-density cups.

Our study demonstrates that some of the size and shape variability of fossils on bedding planes can be explained by population density, an important aspect of intraspecific variability in Spinicaudata.

Acknowledgments: We acknowledge assistance in the field and laboratory by Jan Schmidt, Freie Universität Berlin, and Sarah Sheldon, The University of Akron. Also, we thank Melanie Hopkins, American Museum of Natural History, for discussion and Christopher Rogers, Kansas Biological Survey, for his helpful manuscript review.

Authors' contributions: Study design, data collection, analyses, writing, and revision by MH and SCW.

Competing interests: The authors declare that they have no conflicts of interests.

Availability of data and materials: Supplementary Materials can be downloaded from page 18 and also from the website.

Consent for publication: All authors consent to the publication of this manuscript.

Ethics approval consent to participate: Not applicable.

REFERENCES

Astrop TI, Sahni V, Blackledge TA, Stark AY. 2015. Mechanical properties of the chitin-calcium-phosphate "clam shrimp" carapace (Branchiopoda: Spinicaudata): implications for taphonomy and fossilization. J Crustacean Biol **35:**123–131. doi:10.1163/1937240X-00002332.

Brown BP, Astrop TI, Weeks SC. 2014. Post-larval developmental dynamics of the spinicaudatan (Branchiopoda: Diplostraca) carapace. J Crustacean Biol **34:**611–617. doi:10.1163/1937240X-00002260.

Brown D, Rothery P. 1993. Models in biology: mathematics, statistics and computing. John Wiley & Sons, Hoboken, New Jersey, USA.

Burnaby TP. 1966. Growth-invariant discriminant functions and generalized distances. Biometrics **22:**96–110.

Chen P, Shen Y. 1981. Paleogene conchostracan faunas of China. Geol S Am S **187:**193–202.

Crampton JS, Haines AJ. 1996. Users' manual for programs Hangle, Hmatch, and Hcurve for the Fourier shape analysis of two-dimensional outlines. Institute of Geological & Nuclear Sciences, Science Report.

Defretin-Lefranc S. 1965. Etude et révision de Phyllopodes Conchostracés en provenance d'U.R.S.S. Annales de la Société Géologique du Nord **85:**15–48.

Gallego OF, Mesquita MV. 2000. First record of oligocene conchostracans (Tremembé formation, Taubaté Basin) from São Paulo, Brazil. J S Am Earth Sci **13:**685–692. doi:10.1016/S0895-9811(00)00048-1.

Haines AJ, Crampton JS. 2000. Improvements to the method of fourier shape analysis as applied in morphometric studies. Palaeontology **43:**765–783. doi:10.1111/1475-4983.00148.

Hammer Ø, Harper D. 2006 Paleontological data analysis. Blackwell Publishing, Oxford, UK.

Hammer Ø, Harper DAT, Ryan PD. 2001. PAST: Paleontological statistics software package for education and data analysis. Palaeontol Electron **4:**1–9.

Hethke M, Fürsich FT, Jiang B, Wang B, Chellouche P, Weeks SC. 2019. Ecological stasis in Spinicaudata (Crustacea, Branchiopoda)? Early Cretaceous clam shrimp of the Yixian Formation of north-east China occupied a broader realized ecological niche than extant members of the group. Palaeontology **62:**483–513. doi:10.5061/dryad.9387k41.

Huang W, Chou L. 2015. Temperature effect on development and reproduction of the androdioecious clam shrimp, *Eulimnadia braueriana* (Branchiopoda: Spinicaudata). J Crustacean Biol **35:**330–338. doi:10.1163/1937240X-00002336.

Huang W, Chou L. 2017. Temperature effects on life history traits of two sympatric branchiopods from an ephemeral wetland. PLoS ONE **12:**e0179449. doi:10.1371/journal.pone.0179449.

Ishikawa C. 1895. Phyllopod Crustacea of Japan. Zoological Magazine 7, no. **76:**13–21.

Jackson DA. 1993. Stopping rules in principal components analysis: a comparison of heuristical and statistical approaches. Ecology **74:**2204–2214. doi:10.2307/1939574.

Jones TR. 1862. A monograph of the fossil Estheriae. Monographs of the Palaeontographical Society **14:**1–134.

Packard AS. 1871. Preliminary notice of new North American Phyllopoda. Am J Sci **2:**108–113.

Rohlf FJ. 1990. Morphometrics. Ann Rev Ecol Syst **21:**299–316.

Rohlf FJ, Bookstein FL. 1987. A comment on shearing as a method for "size correction". Syst Zool **36:**356–367.

Schwentner M, Rabet N, Richter S, Giribet G, Padhye S, Cart J, Bonillo C, Rogers DC.2020. Phylogeny and Biogeography

of Spinicaudata (Crustacea: Branchiopoda). Zool Stud **59:**44. doi:10.6620/ZS.2020.59-44.

Stigall AL, Plotnick RE, Park Boush LE. 2017. The first Cenozoic spinicaudatans from North America. J Paleontol **91:**467–476. doi:10.1017/jpa.2017.15.

Tasch P. 1987. Fossil Conchostraca of the southern hemisphere and continental drift, paleontology, biostratigraphy, and dispersal. The Geological Society of America Memoir **165:**1–290.

Timms BV, Richter S. 2009. The clam shrimp *Eocyzicus* (Branchiopoda: Spinicaudata: Cyzicidae) in Australia. J Crustacean Biol **29:**245–253. doi:10.1651/08-3029R.1.

Wang S, Hethke M, Wang B, Tian Q, Yang Z, Jiang B. 2019. High-resolution taphonomic and palaeoecological analyses of the Jurassic Yanliao Biota of the Daohugou area, northeastern China. Palaeogeography, Palaeoclimatology, Palaeoecology **530:**200–216. doi:10.1016/j.palaeo.2019.05.028.

Weeks SC, Benvenuto C, Reed SK, Duff RJ, Duan ZH, David P. 2014. A field test of a model for the stability of androdioecy in the freshwater shrimp, *Eulimnadia texana*. J Evolution Biol **27:**2080–2095. doi:10.5061/dryad.574s4.

Weeks SC, Bernhardt RL. 2004. Maintenance of androdioecy in the freshwater shrimp, *Eulimnadia texana*: field estimates of inbreeding depression and relative male survival. Evol Ecol Res **6:**227–242. doi:10.1093/beheco/13.4.561.

Weeks SC, Marcus V, Alvarez S. 1997. Notes on the life history of the clam shrimp, *Eulimnadia texana*. Hydrobiologia **359:**191–197.

Weeks SC, Marcus V, Crosser BR. 1999. Inbreeding depression in a self-compatible, androdioecious crustacean, *Eulimnadia texana*. Evolution **53:**472–483. doi:10.1023/A:1003106702451.

Weeks SC, Zofkova M, Knott B. 2006. Limnadiid clam shrimp distribution in Australia (Crustacea: Branchiopoda: Spinicaudata). Journal of the Royal Society of Western Australia **89:**155–161.

Zhang W, Chen P, Shen Y. 1976. Fossil Conchostraca of China. Beijing, Science Press. (in Chinese)

Zucker N, Stafki B, Weeks SC. 2001. Maintenance of androdioecy in the freshwater clam shrimp *Eulimnadia texana*: longevity of males relative to hermaphrodites. Can J Zool **79:**393–401. doi:10.1139/z00-211.

Supplementary Materials

Table S1. *Eulimnadia texana* size measurements and selected ratios. (download)

Table S2. Fourier coefficients of 33 hermaphrodites of *Eulimnadia texana*. (download)

Table S3. *Eocyzicus argillaquus* size variables and selected ratios. (download)

Table S4. Fourier coefficients of 51 individuals of *Eocyzicus argillaquus*. (download)

Table S5. Non-parametric MANOVA of lengths at maturity. Groups represent different population densities/400 ml. None of the pairwise comparisons of mature hermaphrodites are significant, indicating similar lengths at maturity. Juvenile lengths in cup 15 are distinct. There were only two mature individuals in cups 1, 5.1 and 10.2, hence they are not shown here. (download)

Fig. S1. Hermaphrodite size (*PC1* scores of log-transformed linear measurements) by population density. (download)

Fig. S2. Population density effect on shape in *Eocyzicus argillaquus*. Principal component scores on *PC2* and *PC3* of a set of Fourier coefficients. (download)

Fig. S3. Raw survival of *Eulimnadia texana* and *Eocyzicus argillaquus*. (download)

Fig. S4. Sex discrimination based on Fourier shape analysis in *Eocyzicus argillaquus*, 14 females, 29 males. Mean female and mean male shape superimposed. (download)

Fig. S5. Length over time by sex in *Eocyzicus argillaquus*. (download)

Fig. S6. Size by population density of the Late Jurassic *Liaoxiestheria linglongtaensis* on nine bedding planes from the Tiaojishan Formation (n = 692). (download)